J. Membrane Biol. 166, 223–235 (1998)

The Journal of
Membrane
Biology

Neuronal Plasma Membrane Dynamics Evoked by Osmomechanical Perturbations

L.R. Mills, C.E. Morris

[1]Playfair Neuroscience Unit, The Toronto Hospital Research Institute and Department of Physiology, University of Toronto, 11-430 TWH 399 Bathurst St, Toronto, Ontario, Canada M5T 2S8

[2]Neurosciences, Loeb Health Research Institute, Ottawa Hospital, 725 Parkdale Ave, Ottawa, Ontario, Canada K1Y 4E9

Received: 13 May 1998/Revised: 18 September 1998

Abstract. When neurons swell and shrink they extensively reorganize their plasma membrane. A striking aspect of these membrane dynamics is the transient appearance of vacuole-like dilations (VLDs) which, counterintuitively, expand as the neurons shrink. Here, confocal microscopy of cultured molluscan (*Lymnaea*) neurons was used in conjunction with aqueous phase and membrane dyes to examine changing VLD membrane topology as VLDs form, reverse or recover. We show that VLDs start as discrete invaginations at the adherent surface, so VLD and plasma membranes are initially contiguous. Over the next few minutes VLDs expand and penetrate the cytoplasm. At the substratum, the mouths of VLDs develop into irregular annuli of motile adherent processes whereas deeper in the cytoplasm, VLD membrane profiles are smooth. Subsequently VLDs spontaneously shrink; as this recovery proceeds, constriction of the motile VLD mouth leads to the internalization of plasma membrane. Washout experiments with aqueous phase dyes demonstrated that VLD constriction yields *bona fide* vacuoles, i.e., membrane-bound compartments isolated from the external medium. VLDs can also be experimentally eliminated by returning cells to swelling conditions; this reversal process drives membrane back to the surface.

VLD formation and reinternalization of VLD membrane can be seen as aspects of plasma membrane surface area regulation. We postulate that area adjustments, driven by regional membrane tension differences, become noticeable when excessive perturbations overload normal membrane reprocessing steps. Both the changes in VLD membrane topology, and previously established capacitance changes accompanying cell shrinking and swelling, argue that osmomechanically perturbed neurons regulate their surface area as their volume changes.

Correspondence to: C.E. Morris

Key words: Surface area regulation — Cell volume — Membrane tension — Cytomechanics

Introduction

Neurons lead electrically active lives and, to facilitate rapid electrical signaling, limit their plasma membrane capacitance. Where myelination is not an option, capacitance can only be minimized by avoiding excess surface membrane. However, minimizing surface area is risky, as it eliminates any slack on the essentially inelastic lipid bilayer; taut bilayers rupture under increased tension. Thus, neurons have conflicting needs: on the one hand, to minimize surface membrane and on the other, to provide for mechanical resilience of the surface membrane. How neurons resolve this conflict is part of the wider issue of plasma membrane surface area regulation.

Neurons also lead mechanically active lives, and this too creates a demand for cell surface area regulation. Neurites must adhere and generate tension to grow or rearborize and, in the face of endogenous and exogenous forces (*see* Van Essen, 1997), maintain tension at appropriate levels throughout life. Once established, arborizations of a given neuron extend in many directions and may traverse many environments. Axonal transport and membrane cycling keep the cytoplasm mechanically active even when the neuron appears quiescent. Since the lipid bilayer delimiting any cell can expand no more than 3% in area under tension (e.g., Nichol & Hutter, 1996), maintenance of plasma membrane integrity during mechanical events is not achieved by bilayer stretch and recoil. Instead, an adjustment of the quantity of surface membrane is required; how this regulation is achieved is not understood (*see* e.g., Bray, 1996). We suggest (Wan, Harris & Morris, 1995; Reuzeau et al., 1995; Morris, Lesiuk & Mills, 1997) that local membrane tension is both a primary signal and a primary effector in a feedback loop for surface area regulation.

The idea that neurons regulate their surface area stems from two sets of observations: (i) during both swelling and shrinking, membrane capacitance changes roughly parallel the apparent membrane area changes (Wan et al., 1995) and (ii) shrinking stimuli elicit dramatic membrane rearrangements (Reuzeau et al., 1995) in the form of large vacuole-like dilations (VLDs). Neither phenomena (capacitance changes, VLD generation) depend on $[Ca]_{ext}$ or $[Ca]_{int}$ (Herring et al., 1998) and VLD dynamics are insensitive to absolute osmotic and ionic strength. These findings suggest that mechanical forces, rather than chemical changes, associated with swelling and shrinking trigger these membrane rearrangements.

Figure 1 summarizes VLD formation, recovery and reversal as visualized by Hoffman modulation optics (Reuzeau et al., 1995). Formation is the process whereby neurons, previously swollen in hypotonic medium, rapidly form large membranous vacuole-like dilations (VLDs) upon their restoration to normal saline (NS). VLDs are transient; left in NS, they disappear over tens of minutes to hours depending on the severity of earlier swelling stimuli. This cell-mediated disappearance we term VLD ''recovery.'' Experimental interventions that reswell the cell also cause loss of VLDs; this very rapid process (~1 min) we term ''reversal.'' Our working hypothesis is that VLDs form as cells shrink because membrane recruited during swelling (*see also* Sukhorukov, Arnold & Zimmermann, 1993) is now excess and at ''slack tension'' and thus easy to retrieve. Recruitment of new membrane during swelling and VLD formation during retrieval of excess membrane, are ''physical'' or ''passive'' responses wherein the cell structure interacts with exogenous mechanical forces. The subsequent spontaneous elimination of VLDs, during recovery, is ''biochemical'' or ''reactive'' and is impaired by cytochalasin (Reuzeau et al., 1995). This is in contrast to reversal which is cytochalasin insensitive.

In this paper, we use confocal microscopy with fluorescent aqueous phase and membrane dyes to study VLD formation and reinternalization of VLD membrane. We are particularly concerned with the changing topology of VLD membrane, since this directly addresses questions about how cells regulate their surface area. Such regulation is a particularly critical issue for neurons given their capacity for morphological plasticity, yet little is currently known about how they adjust their surface area appropriately during volume and shape changes.

Materials and Methods

Cells and Solutions

Circumoesophageal ganglia were removed from mature *Lymnaea stagnalis* and placed into NS (''normal saline''), an isotonic physiological solution (in mM): 50 NaCl, 1.6 KCl, 3.5 $CaCl_2$, 2.0 $MgCl_2$, 5.0 Hepes, 5.0 glucose; pH 7.6 adjusted with 1N NaOH; gentamicin added at 50 mg/100 ml; osmolarity 126 mosM, and gently agitated with 0.25% type XIV protease (Sigma, St. Louis, MO) in Ca-free NS for 30 min then washed in NS. Neurons were grown on an untreated glass coverslip. One gangion was placed at the edge of each well and teased apart with forceps, thus releasing neurons that settled and adhered. Keeping ganglion debris to a minimum facilitated adhesion. The heterogeneous population of unidentified neurons (*see* Sigurdson & Morris, 1989) rearborized with no growth factors beyond what the remainder of the ganglion itself might release. The neurons had a broad range of morphologies, from heavily arborized, through fried egglike. Experiments were carried out at room temperature (~20°C) 1–4 days after plating.

Solution exchanges were made by hand using Pasteur pipettes. Solutions were made hyposmotic by dilution with distilled water. Approximately 2/3 of the NS was rapidly removed from the dish using a Lieden aspirator and the dish was flooded with distilled water (with or without dye). Typically, cells were exposed to swelling stimuli for 4–5 min. Subsequently the swelling solution was aspirated away and the cells were flooded with NS to evoke formation of VLDs. These neurons are extremely tough in media of low osmolarity (Wan et al., 1995).

Confocal Microscopy

To select individual cells for an experiment and to grossly assess labeling or bath content, cells were viewed on the standard Nikon microscope in transmitted light (phase optics) or epifluorescence mode. However all monitoring of VLD dynamics was done using the confocal microscope. Neurons were viewed with an inverted (Nikon base) scanning confocal microscope (Bio-Rad MRC-600) equipped with an argon-ion laser (Mills et al., 1994), in both phase contrast (transmitted light, nonconfocal) and confocal epifluorescence modes using a 60× planApo objective. An adjustable pinhole in the detector lightpath controlled the optional section thickness and illumination intensity was controlled by a filter wheel. A neutral density filter of 2 or 3 was used on all preparations. To visualize neurons in the presence of Lucifer Yellow (LY), the fluorescein filter set was used and for Rhodamine-Dextran 3000 (RD3000), and 1,1′-dioctadecyl-3,3,3′,3′-tetramethylindocarbocyanine perchlorate (Dil) the rhodamine filter block. To follow the appearance of the VLDs, single confocal images were collected every 2–60 sec (but usually 10–15 sec). In many cases, simultaneous fluorescent and phase contrast images of the cells were taken using the second channel to collect the (non-confocal) transmission images. VLD formation was also monitored by optically sectioning neurons; in this case optical series were taken using a single scan per section and step sizes (the distance between two optical sections) of 0.5–3.0 μm.

Labeling of VLDs with Aqueous and Membrane-Soluble Fluorescent Dyes

The fluorescent compounds RD3000 (dextran of molecular weight ~3000 conjugated to tretramethylrhodamine), LY, and Dil, all from Molecular Probes, OR were used in conjunctions with fluorescent microscopy to monitor VLD formation, recovery and reversal. In most cases neurons were also monitored intermittently with phase optics. LY (final concentration 100 μM) or RD3000 (final concentration 25 μM) was added to the bath just prior to the first osmotic perturbation and the concentration was thereafter maintained in all the rinsing solutions unless noted. In the presence of either dye, neurons were not visible using conventional epifluorescence microscopy due to the intense signal from the out-of-focus fluorescence. In contrast, in the

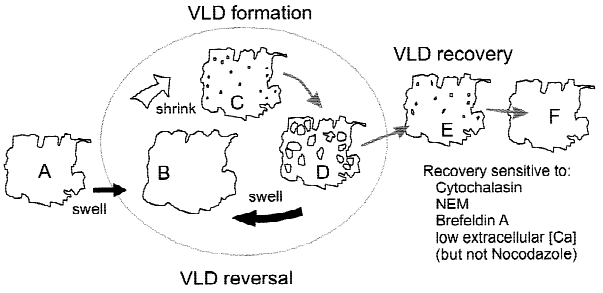

Fig. 1. Overview of VLDs. Schematic showing how vacuole-like dilations (VLDs) are induced and undergo recovery or reversal as visualized by Hoffman Modulation optics (Reuzeau et al., 1995). Inhibitors of VLD recovery are listed; they do not interfere with VLD formation and reversal. A neuron (*A*) swells (straight black arrow) when saline is diluted (~4 min) (*B*) and shrinks (white arrow) on return to normal saline (NS). As the neuron continues to shrink, membranous dilations appear (*C*) and enlarge (*D*) — this is VLD formation. If the neuron is made to reswell (curved black arrow) the VLDs reverse (i.e., rapidly shrink and disappear, expelling their contents). Cycles of swell/shrink-induced VLD formation and reversal (encircled) can be repeated. Or, if a VLD-bearing neuron is left undisturbed in NS (series of grey arrows) its VLDs disappear in tens of minutes or a few hours, depending on the extent of prior osmotic insults. This ''spontaneous'' disappearance — recovery — is accompanied by churning motor activity in the cytoplasm.

confocal microscope, the out-of-focus fluorescence was eliminated and the neurons were readily visible as black objects against a bright background. Dil in ethanol or in DMSO (final concentration 2.5 μM) was used to label the plasma membrane. In this case the dye was added briefly (<30 sec) to the bath during the swelling phase where it permanently labeled the cell membrane; the bath signal was washed out by return to Dil-free medium.

Results

Neurons form VLDs in Response to Osmotic Perturbations

VLD formation is not haphazard during repeated swell/shrink cycles. As illustrated in phase contrast images (Fig. 2*a*(A–D)), individual VLDs exhibit a signature shape, size and location at each reappearance. This cell typifies neurons stained with Dil then monitored by confocal microscopy in both transmitted and fluorescence modes. Laser illumination of the intensity and durations employed did not detectably impair the capacity for VLD formation and reversal. Repeated laser scans during recovery may, however, have slowed this complex drug-sensitive (*see* Fig. 1) process.

We postulate that VLD phenomena reveal exaggerated aspects of surface area regulation and, on that basis, we address the following questions: (i) Are VLDs initiated as plasma membrane invaginations or alternatively, endomembranous vesicles that dilate and then acquire bath dye by fusion to plasma membrane? and (ii) If VLDs start as plasma membrane invaginations, not as true vacuoles, can the VLD membrane nevertheless eventually be reinternalized?

VLD Topology Revealed by Imaging VLD Contents

Fig. 2*b*(A–C) shows VLDs as visualized by aqueous phase dye in their lumen. In these experiments, the confocal microscope's ability to reject the out-of-focus fluorescence signal from the bath was essential. RD3000 concentration was held constant during all osmotic perturbations consequently the neuron appeared as black against the intense bath signal. VLDs imaged via their fluorescent aqueous contents behaved as expected from VLDs monitored by transmitted light; they rapidly formed (<1 min) within the bounds of the cytoplasm when neurons shrank, then vanished (reversal) when neurons were made to reswell. RD3000-filled VLDs subsequently reappeared (compare A and C) when the swollen cells were shrunk a second time in NS. Fluorescent VLD profiles occurred at the same locations in the second round of NS (*see* arrows), with the addition of some new VLDs. During reversal, the aqueous phase dye signal rapidly diminished to nothing. It did not shrink and intensify as would be expected if reversal constituted the compression of a dilated endomembranous vacuole.

To determine if VLDs ultimately pinched off to become true vacuoles, i.e., dye-retaining compartments, we followed the fate of RD3000-labeled VLDs during recovery in the presence and absence of bath dye. Fluorescence images taken within 120 sec of VLD initiation (Fig. 3*A–E*) showed multiple RD3000-labeled VLDs of diverse size and shape inside neurons bathed in a sea of RD3000, indicating that at this time the VLD lumen and the bath were contiguous, and suggesting that invaginating plasma membrane is the source of VLD membrane. The RD3000/NS bath was then exchanged for dye-free NS (Fig. 3*F–I*). Phase contrast images during the next 3–10 min show the location of multiple VLDs (where not obscured by the soma), but cannot reveal which ones, if any, have pinched off. Comparison with the simultaneous fluorescence images reveal that there are two populations of VLDs, those that retain the dye, indicating that they have have pinched off (*see* arrows) and those that lose the dye during washout through a still-patent opening to the bath. Because VLDs in the latter population are empty of fluorescent dye, they can only be identified in the phase panel (e.g., *see* phase and fluorescence images in *G*).

Typically the vacuolization of VLDs began within minutes of VLD formation. A washout time-series for a single neuron (Fig. 3*J–M*) demonstrates that, at any given time during recovery, progress towards vacuolization (pinching off) varied even among neighboring

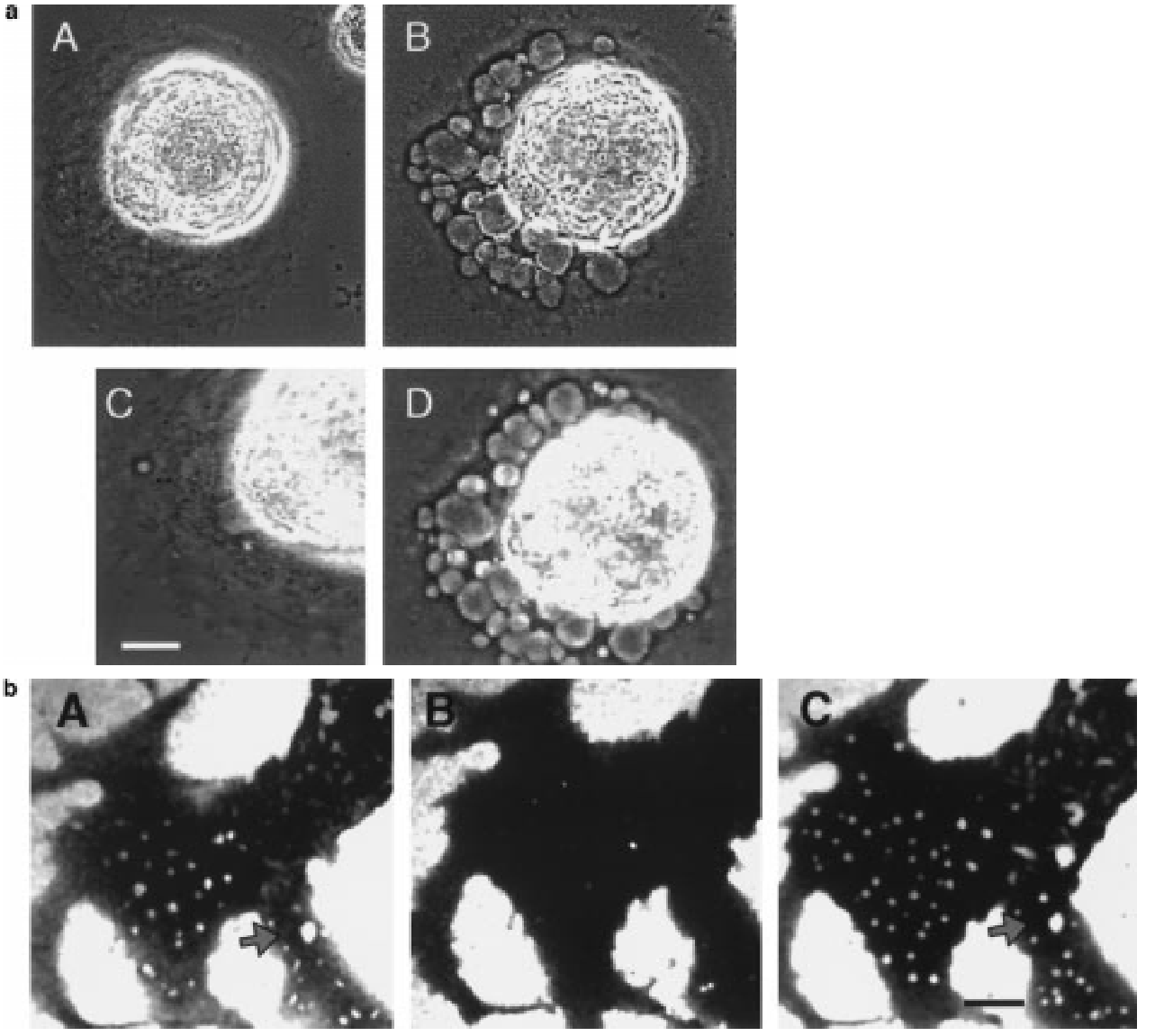

Fig. 2. VLDs form repeatedly at discrete sites. (*a*) Phase contrast images showing discrete VLDs generated during successive swell/shrink cycles; *A,* in NS, *B,* 9 min later after a swell/shrink stimulus (4 min swell, 5 min in NS) multiple VLDs are visible. *C,* 10 min later (10 min swell) the VLDs have reversed; *D,* 6 min after switching back to NS (and 25 min after *A*) large VLDs have reformed. Comparison of *B* and *D* shows that a few VLDs are new, but most reoccur at previous sites and show a reproducible size and shape, as if delimited by a robust membrane skeleton. Scale bar: 12 μm. (*b*) Fluorescence images using RD3000 in the bath showing VLDs reforming at discrete sites, having expelled their contents between shrink episodes. *A,* numerous fluorescent VLDs are visible inside a cell that has undergone a prior swell/shrink cycle. The arrow points to VLDs in *A* that will reappear at the same site in *C.* The cell appears black against intense signal from RD3000 in the bath. *B,* after a second swell stimulus, most VLDs have disappeared but in *C,* with the cell switched back to NS, they reappear, principally with the same size and location (compare *A* and *C*). Scale bar: 13 μ.

VLDs. Here, two VLDs retained dye whereas two adjacent VLDs gradually faded over the next 80 sec, as their luminal contents slowly equilibrated with the nonfluorescent bath presumably because they were not fully pinched off during the time of observation. Such differential dye loss in adjacent VLDs was common and indicates that the restriction to diffusion in and out of VLDs was a feature of an individual VLD, not of the pathway between the VLD mouth and the bulk of the bath. Comparable results were obtained using Lucifer Yellow or carboxyfluorescein in the bath.

VLD Topology Revealed by Imaging VLD Membrane

If VLD contents are initially contiguous with the bath, VLD membrane must initially be contiguous with

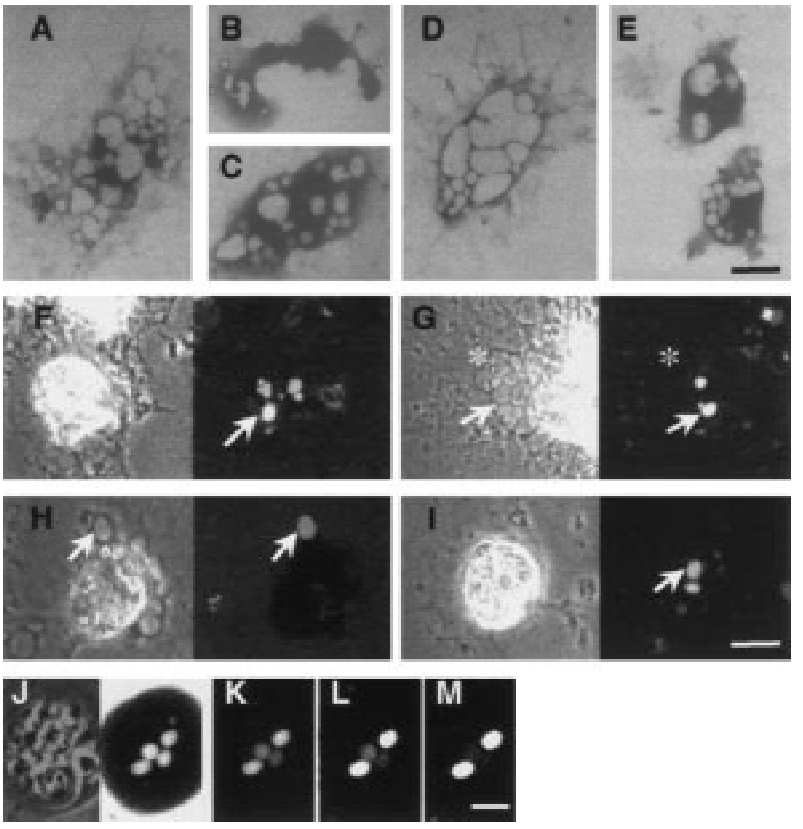

Fig. 3. VLD topology revealed by an aqueous phase dye. [*A–E,* Fluorescence images of cells given a swell/shrink cycle with RD3000 continuously present in the bath. All images were obtained <1 μm from the substratum within 3 min of switching back to NS (''shrink''). RD3000-filled VLDs of diverse size and shape are apparent inside the neurons that appear dark against the bath signal. 10 min after VLD formation, RD3000 was washed (isosmotic) from the bath. *F–I,* phase and corresponding fluorescent image pairs, were obtained over the next 3–10 min. White arrows identify VLDs that retained dye after washout (arrows are absent in the phase images of *F* and *I* because VLDs under the soma cannot be detected in phase). *G,* asterisks in the phase and fluorescent images label a site where multiple VLDs are visible in phase but not in the corresponding fluorescence image, having lost dye during washout (see text). *J–M,* a single neuron with VLDs at different stages of pinching off: *J,* phase and fluorescent images immediately prior to washout, *K, L,* and *M* immediately after washout (~10 sec later), 25 sec and 80 sec later, respectively. The lumenal content of two VLDs equilibrates with the non-fluorescent bath (hence their VLD profiles de-intensify then disappear whereas the other two stay bright). Scale bars: *A–I* 10 μm, *J–M* 6 μm.

plasma membrane. Confocal microscopy of the plasma membrane in the plane of the substratum should, therefore, reveal the early mechanics of VLD initiation. Trials with different membrane dyes indicated that these dynamic events were most easily captured with exclusive plasma membrane staining (Fig. 4 and subsequent figures); whenever dyes rapidly stained the plasma membrane and endomembranes, distinguishing VLD membranes from organellar membrane was difficult. Trial and error showed that adding DiI in ethanol to swollen neurons just prior to a shrinking (VLD-eliciting) stimulus yielded the best chance to selectively stain the plasma membrane. Unfortunately, however, this protocol afforded no opportunity to image the membrane prior to the swell stimulus.

Neurons were stained during minutes 3–4 of a 5-min swelling stimulus, using DiI in ethanol (or in some cases ''fast'' DiI in DMSO) added to distilled water to give a final concentration of 2–5 μM. Because of the aqueous insolubility of DiI, a fine DiI suspension formed. A 60-sec exposure to DiI was followed by repeated washing in DiI-free swelling medium to eliminate the bath signal. Even after washing, intensely fluorescent precipitated DiI particles littered the substratum e.g., Figs. 4 and 5. Not surprisingly, staining intensity varied substantially among cells. After returning to NS (the shrinking stimulus) and quickly adjusting focus, the substratum plane was continually monitored (~2-sec intervals) in order to capture the earliest stages of VLD formation.

VLD Initiation

Figure 4*A* shows the plasma membrane footprint of a swollen cell immediately after labeling with DiI. Although the plasma membrane at the substratum showed some staining inhomogeneities, no ''pre-VLD'' structures could be discerned. In other words, once VLD locations were known, back-extrapolation to preshrinking images revealed no specializations at the VLD loci. By 45 sec after the return to NS the first signs of VLD formation, points of increased staining intensity were visible (*See* Fig. 4*B*). Over the next minute, these initiating ''spots'' expanded, acquiring an annular appearance (Fig. 4*C–E*). As the annuli intensified, their midregions darkened, consistent with invaginating and dilating membrane being drawn deeper into the cytoplasm, beyond the confocal plane. Comparison of the phase and fluorescent images (Fig. 4*F–G*), confirmed that the DiI-labeled annuli corresponded to VLDs. With time, the expanding annuli became increasingly ragged at the substratum adhesion plane (Fig. 4*H*). This ragged appearance did not, however, extend far in the Z-direction; little more than 1 μm above the substratum, the VLD profiles

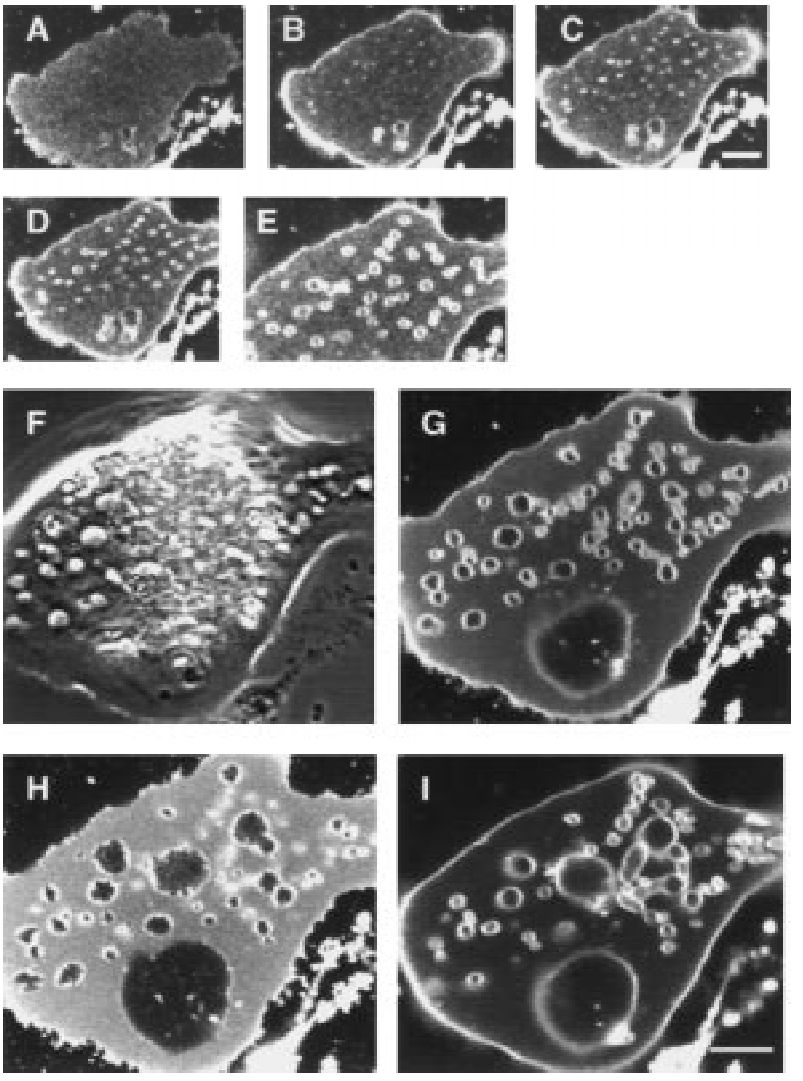

Fig. 4. VLD formation in a Dil-labeled neuron. Panels *A–E*, fluorescent images of a Dil-labeled neuron, over a period of ~2 min during VLD initiation; Dil as previously rinsed from the bath. At 10 sec post return to NS no VLDs are visible (*A*) but by 45 s (*B*) VLDs are evident as small points of intense fluorescence in the plasma membrane adjacent to the substratum. Over the next 90 sec (*C–E*) these points expand (*see* text). In *F* and *G*, one min later simultaneous phase/fluorescence images at the substratum show that the rapidly invaginating membrane corresponds to VLDs. *H* and *I* fluorescence images of two slices from a Z-series taken immediately after *F*, *G* and *I* is 2.5 microns above *H*. They illustrate marked differences in VLD morphology near the substratum and deeper in the cytoplasm. Scale bar: *A–D* 13 μm (*E* is zoomed 1.5× relative to *A–D*), *F–I* 10 μm.

were smooth and round, as illustrated by Fig. 4*I*, which is 2.5 μm above Fig. 4*H*).

Stepping up from the substratum in a Z-series, the smooth Dil-stained profiles continued until the VLDs ended blindly in the cytoplasm. VLD height and shape varied. Several microns above the substratum, some VLDs became multi-lobed (compare Fig. 4*H–I*). Where cytoplasm was deeper (e.g., in somata rather than in lamellae) VLDs tended to invade further; >5 μm into the cytoplasm was common in somata.

VLD RECOVERY

Aqueous phase and membrane dyes provided complementary information about VLD dynamics associated with recovery and vacuolization. Z-series during early recovery readily confirmed that RD3000 fluorescence in VLD lumens terminated blindly in the cytoplasm (*not shown*). At the substratum, however, obtaining structural or dynamic information relevant to dye retention was difficult. Only occasionally did the RD3000 profile at the substratum reveal any structural complexity, presumably because the ragged annuli, vividly and invariably revealed with Dil-labeling (e.g., Fig. 5) were too thin to be imaged as negative volumes with bath dyes.

Comparison of Figs. 4 and 5 reveals that as neurons progressed from VLD formation through recovery the plasma membrane delimiting the mouths of the VLDs changed markedly. The originally simple rings of Dil-labeled membrane observed during VLD formation (Fig. 4) were transformed into extravagantly ragged structures during recovery (*see* Fig. 5). During the transition from VLD initiation/formation to VLD recovery, the initial outwardly directed widening of the VLD mouth gave way to a centripetally directed creeping of the ragged edges. Eventually, these inward motions obliterated the

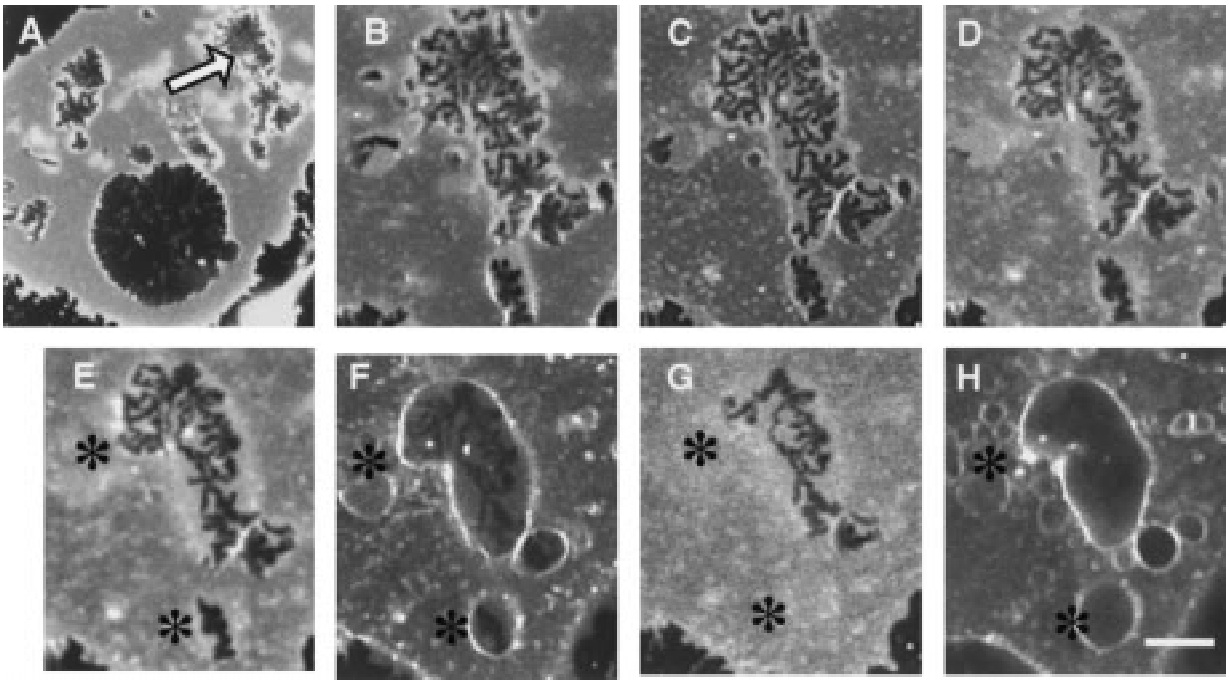

Fig. 5. VLD recovery in a Dil-labeled neuron. *A–H* fluorescence images of the same neuron as in Fig. 4 (compare Fig. 4*H* with Fig. 5*A*), over a 30-min period illustrate the process of recovery. (*A*) 10 min after Fig. 4*H* some VLDs visible in Fig. 4*H* have closed off but others have increased in size; the arrow in *A* indicates the area images at higher resolution in subsequent panels, (*B–H*). All images are at the substratum plane except *F* and *H*, which are 1 and 1.5 μm up. In *B*, 10 min after *A*, recovery is well underway; actipodia (*see* text) are visible within the central portion of the VLD mouths. Over the next 20 min the actipodia are motile and the VLD mouths shrink and some close (*see C* through *H*). Once a VLD mouth closes, all signs of the VLD disappear at the substratum; in *E*, 15 min after *B*, the upper asterisk labels such a site whereas the lower asterisk labels an open VLD mouth. (*F*) 3 min after *E*, at a confocal plane above the substratum, both VLD profiles remain visible (*see* asterisks). (*G*) 2 min later all signs of both the VLDs labeled in *E* and *F* have vanished at the substratum yet both are still visible above the substratum in *H*, which is 5 min after *G*. Thus, the VLDs have been pinched off and their membrane re-internalized. Scale bar: 6 μm.

VLD mouths and are presumably what ultimately creates true vacuoles.

In some VLDs, the plasma membrane that elevated from the substratum as VLDs formed seemed to simply subside again during recovery; these likely corresponded to VLDs that, in Hoffman optics ''faded'' (Reuzeau et al., 1995) rather than progressively shrank. However, Dil images in the Z direction showed unequivocally that the fate of many VLDs during recovery was constriction and ultimate vacuolization. For example, inspection at the substratum (Figs. 4*H*, 5*E* and *G*) and deeper into the cytoplasm (Fig. 4*I*, 5*F* and *H*) shows smooth bubblelike VLD membrane profiles above both partially and fully constricted annuli. This mix is what is predicted from the RD3000 washout experiments (Fig. 3*F–M*).

Monitoring the Dil-labeled substratum-adherent membrane over time made it clear that this region was extremely motile during recovery. VLD recovery is cytochalasin-sensitive (Reuzeau et al., 1995); and filamentous actin quickly reassembles in the motile annuli of recovering VLDs (Cohan et al., 1997; Herring, 1998). Consequently we termed these actin-rich structures *actipodia.* During recovery, the most dramatic actipodial behavior revealed by Dil (the formation of multiply branched motile protrusions) occurred at the largest VLD mouths. Smaller VLDs, which typically recovered and pinched off earlier than large ones, exhibited more circumspect actipodial activity. In the 30-min time series shown in Fig. 5, all but the largest VLD mouths have become occluded (compare *B* and *G*). Once a VLD mouth was closed (e.g., asterisks in Fig. 5*E* and *G*) all signs of the VLD disappeared on the substratum-adherent plane, yet, in focal planes just above the substratum, the dilated VLDs remained clearly evident (e.g., asterisks in Fig. 5*F* and *H*). Such VLDs had become true vacuoles. Other VLDs, with mouths only partly occluded, had much larger dilated lumens in planes above the substratum as if they too would ultimately pinch off (vacuolate).

During recovery, intense Dil staining close to the margins of constricting VLDs was a consistent feature. This was first apparent at the substratum (*see* Fig. 5*B*), but as recovery proceded the intensely stained rims were generally more evident in confocal plane a micron or two in the Z direction (*see* Fig. 5*F* and *H*). This staining pattern may reveal zones of endocytic membrane re-

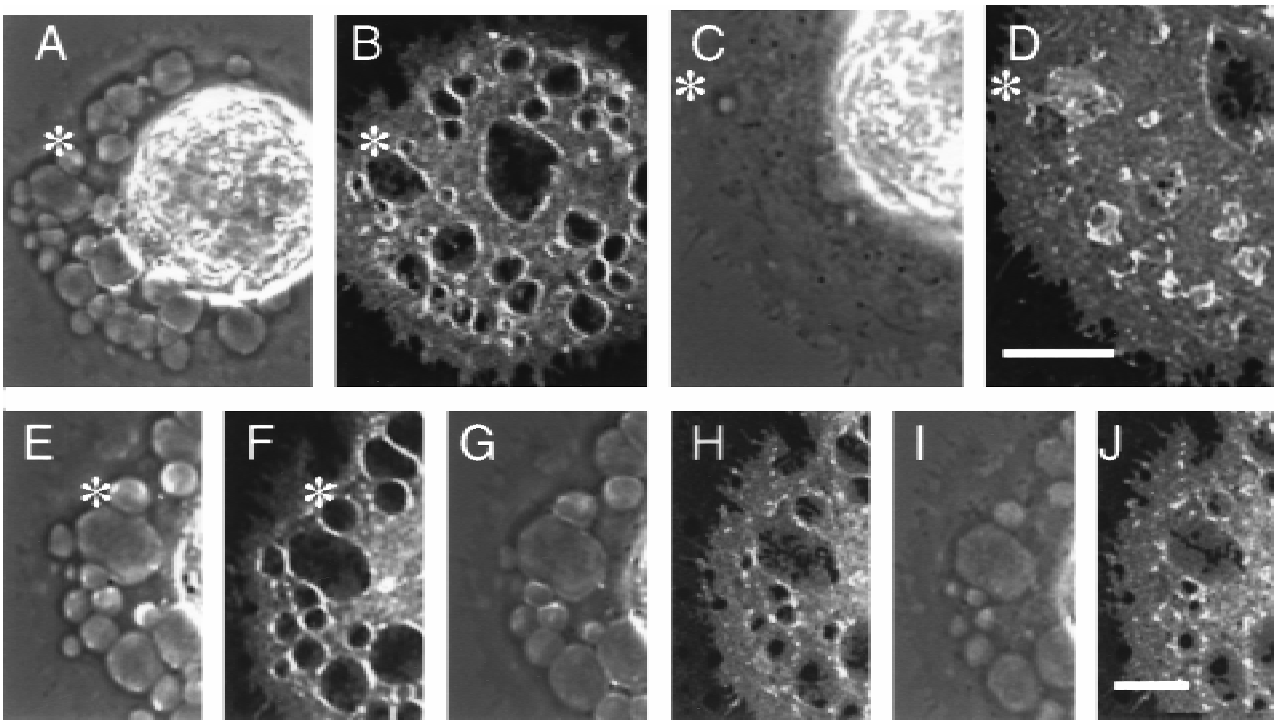

Fig. 6. Using a membrane dye to monitor VLD reversal. Simultaneous phase and Dil fluorescence images of the neuron shown in phase only in Fig. 2*A* during multiple cycles of swelling-induced reversal. All images are at the substratum, except for *C* and *D* which were focused at a marginally different plane (0.1–0.2 μm) up from the substratum to emphasize the compacted VLD membranes (*see* text). The first round of VLDs were evoked by the usual swell shrink cycle (*not shown*). 10 min later, panels *A–D,* reversal was induced by swelling the cell. (*A* and *B*) At 60 sec into reversal. VLDs in phase and fluorescence images correspond; the white asterisk labels one of many VLDs visible in both images. (*C* and *D*) By 8 min reversal is essentially complete in the phase image (*see* asterisk in *C*) but incomplete as assessed by Dil (*see* asterisk in *D*) in the fluorescent image (*see* text). After 10 min of reversal another cycle of VLD formation and reversal, panels *E–J,* is initiated. (*E* and *F*) 10 min after the return to NS. The white asterisk labels one of many newly formed VLDs similar in size and shape to those observed in cycle 1 (compare *A* and *B*). (*G* and *H*) And 3 min into reversal (and 4 min after *E* and *F*) Dil-labeled VLDs mouths are closing at the substratum but the membranous invaginations deeper in the cytoplasm (evident in the phase image) are largely unchanged. (*I* and *J*) 7 min later VLD mouths are nearly closed but those VLDs which have not yet compacted remain evident in the phase image. Scale bars: *A* and *B,* 12 μm; *C* and *D,* 10 μm; *E–J,* 8 μm.

trieval. Whatever process is responsible, it occurred in both pinched-off VLDs (vacuoles) and in still-patent VLDs (invaginations), as seen by the staining patterns in Fig. 5*F* and *H.*

VLD Reversal and Repeatability

The cell-mediated events of recovery lead, without experimental intervention, to VLD disappearance. Newly-elicited VLDs can, however, be made to rapidly disappear by reswelling of the cell. This physically mediated ''reversal'' is a defining attribute of VLDs and is insensitive to drugs and levels of extracellular calcium (*see* Fig. 1; Herring et al., 1998).

Observations with RD3000 suggested that during reversal VLDs expelled their lumenal contents to the bath (Fig. 2*B*), but what becomes of the membrane? Fig. 6*A–D* follows VLD membrane in a Dil-labeled cell during reversal. When reswelling of the cell has just begun, simultaneous phase fluorescence image pairs show brightly fluorescent rings of Dil-labeled membrane (*see* Fig. 6*B*) closely aligned with the VLDs visible in the phase image (*see* Fig. 6*A*). An exception is the VLDs under the soma which are obscured in the phase images, e.g., the large central VLD in Fig. 6*B.* However images taken later, when reversal is well underway, reveal striking differences between phase and fluorescent images. Whereas reversal appears essentially complete as assessed by the phase image (Fig. 6*C*), the simultaneous fluorescence image (Fig. 6*D*) still reveals multiple VLD sites evident as either small mouths or intensely Dil-labeled material. These structures, barely apparent in phase contrast, were presumably VLD membranes compacted and compressed towards the substratum. Consistent with this interpration was the loss of VLD structure in fluorescence images from focal planes above the substratum (*not shown*). Typically, complete ''Dil-reversal'' was considerably slower than was evident from phase contrast images (or from Hoffman Modulation; *see* Reuzeau et al., 1995), and in some cases tens of minutes were required.

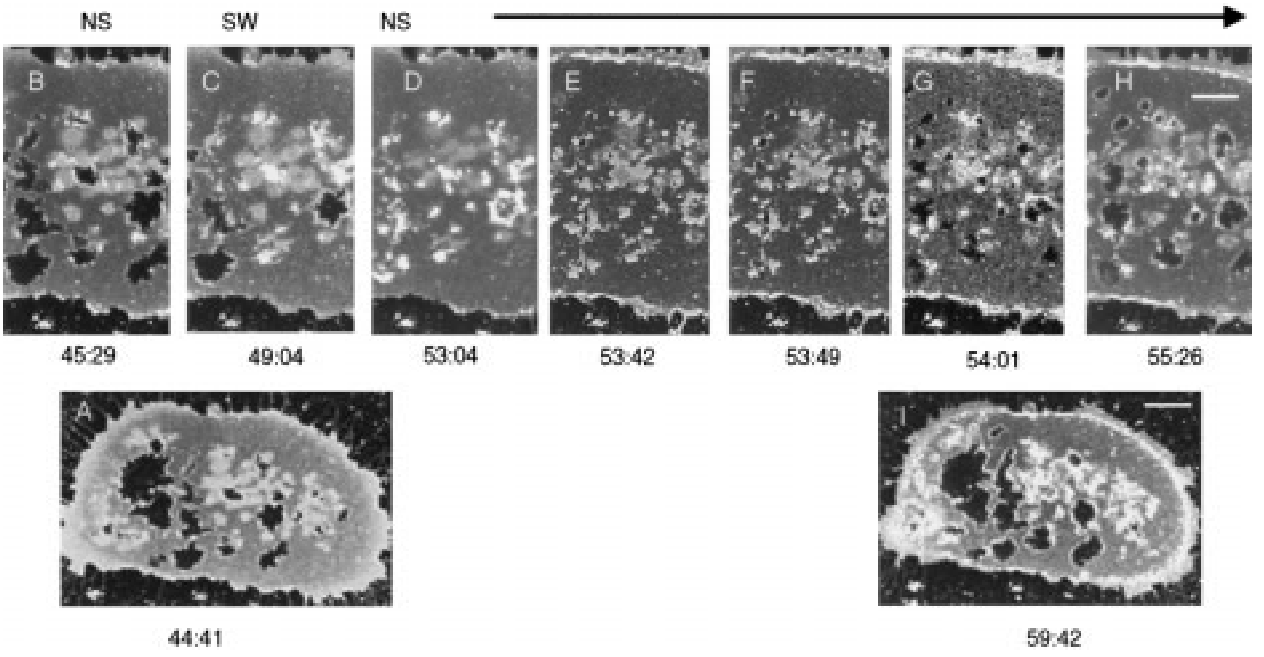

Fig. 7. Persistence of the cell margin and of precise VLD sites. Fluorescence images of a Dil-labeled cell during the second and third of a 3-cycle swell/shrink cycles; the time in minutes from the start of the experiment are given under each panel, all images are at the substratum. (*A*) The cell footprint in NS, late in the second cycle of VLD formation. *B–H* shows part of the cell during the next swell/shrink cycle: *B,* VLD mouths are open at the substratum; *C,* the saline is diluted (''SW'' ell) and VLDs are reversing; *D,* immediately after return to NS, no new VLDs are apparent, but 38 sec later (*E*) VLD initiating sites appear. Though recently disturbed, the substratum plasma membrane does not simply lift; VLDs in a second cycle are initiated as small discrete ''mouths''. (*F* and *G*) Over the next 19 sec. the VLDs rapidly enlarge; many are at VLD sites from the earlier cycle. (*H*) 85 sec later many of the VLDs are similar to those seen in the previous cycle (*see B*). (*I*) The cell footprint in the third cycle. Scale bars: *A* and *I,* 16 μm; *B–H,* 10 μm.

To emphasize the repeatability of VLDs, Fig. 6*E–J* follows the same cell during a second cycle of VLD formation, this time catching reversal before the VLD membrane has compressed to the substratum. Fig. 6*E* and *F* shows that during the second round of VLD formation, VLDs imaged in simultaneous fluorescent and phase images coincide and are similar in size, shape and site of origin to those formed in the first cycle (compare Fig. 6*A* and *B*). During reversal (Fig. 6*G–J*) the VLDs as visualized with Dil (*H* and *J*) close in at the substraum at variable rates. The asterisk in Fig. 6*E* and *I* identifies a large VLD mouth that gradually closes in the fluorescent images but appears little changed from pre-reversal (Fig. 6*E*) in the simultaneous phase images. Over the same time span (7 min), however, other smaller VLDs shrink and vanish in both fluorescence and phase image pairs. Subsequent to Fig. 6*I* and *J* the large VLD, too, collapsed in the fluorescence image (as in *D* of the previous cycle) and vanished in the corresponding phase image (as in *C, data not shown*). Throughout these multiple cycles of VLD formation and reversal it is striking that, despite the severity of the osmomechanical stimuli and membrane reorganization that they engender, the margins of the cell show little disruption.

Figure 7, which shows a Dil-labeled cell undergoing cycles 2 and 3 of a 3-cycle swell/shrink series, illustrates in more detail the reproducibility of VLD formation sites. Figure 7*A* is the 'footprint' of the entire cell, late in VLD formation; Figure 7*B–H* follow the fate of VLDs in the central region of the cell over the next 10 min as VLDs first reverse when swelling medium is added (Fig. 7*C*) and subsequently reform with the application of NS in (Fig. 7*D–I*). In Fig. 7*C* the VLDs observed in Fig. 7*B* had shrunk and in some cases the VLD mouths had closed completely. ''Collapsed'' or compacted VLD membrane as noted previously in Fig. 6*D* was also evident. After all VLD mouths had closed, the cell was switched again to NS. Fig. 7*D* shows the cell in NS just prior to any detectable new VLD openings; Fig. 7*E* was 38 sec later when small dark openings indicated where VLDs were forming anew. VLD formation proceeded rapidly over the next 19 sec (Fig. 7*E–G*). By 85 sec later (Fig. 7*H*) the general size and shape of the VLD mouths roughly paralleled that of the VLD mouths observed in the prior cycle (compare Fig. 7*H* and *B*) but as usual, new VLDs had also been recruited (compare also Fig. 7*A* and *I*). Inspection of the cell footprints (Fig. 7*A* and *I*) during the two separate cycles of VLD formation again illustrates that extensive membrane reorganization can occur at VLDs while overall cell morphology is preserved.

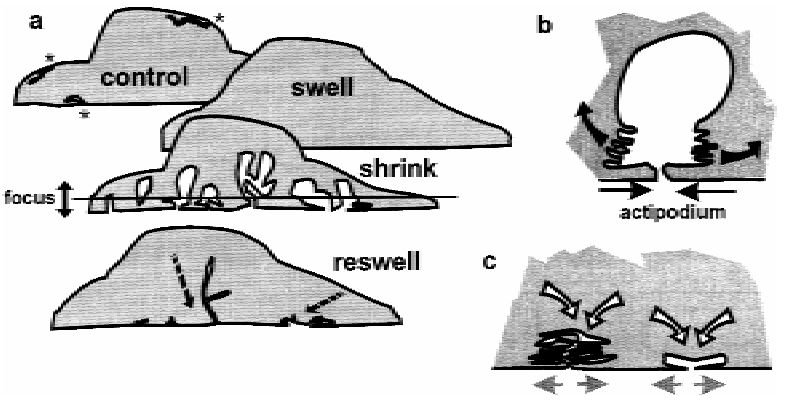

Fig. 8. Interpreting VLD topology during formation, reversal and recovery. (*a*) Idealized Z-planes for a cell undergoing osmotic perturbations. Membrane stores recruited during swelling (asterisks) are putative. Confocal planes near the substratum (double arrow) reveal VLDs in various states of development, from newly initiated to partially and fully pinched off. During reswelling, the VLD membrane and contents disappear (dashed arrows). (*b*) An interpretation of a VLD in recovery; net retrieval is suggested by the curved arrows. Actipodia advance centripetally, forming a constriction (straight arrows). (*c*) Interpretations of Dil images of VLDs undergoing reversal, with VLD membrane compressed (white arrows) at the substratum. If there is a net outflow of VLD membrane during reversal, bilayer material would flow via the substratum plasma membrane, as indicated (grey arrows).

Discussion

Confocal microscopy showed that VLDs (imaged by a membrane dye) invaginated from discrete points at the substratum-adherent surface. Although the adherent cell margins were remarkably stable, the mouths of the VLD invaginations rapidly (minutes) became flamboyant-looking with motile processes (the motile mouths we term actipodia). Constriction of actipodia was responsible for pinching off some VLDs (aqueous dye experiments), and thus for reinternalization of excess plasma membrane. Thus, where neuronal membrane contacted the substratum, a given osmomechanical stimulus produced a spatially diversified response: while the cell margins held firm, the region behind the margins formed VLDs and generated diverse-sized motile actipodia. Membrane and actin dynamics are often studied at dorsal surfaces of cultured cells, making it possible to overlook events at the adherent surface, our primary emphasis. In vivo, however, neurons adhere to various substrata over most of their surface; this adds to the interest of what is seen here of the adherent surface's capacity for mechanically driven and cell-mediated membrane dynamics.

Figure 8*a* encapsulates VLD topology and dynamics as gleaned from confocal microscopy of the live neurons. Idealized Z-planes provide an interpretation of our observations as neurons swelled, shrank, underwent VLD formation and early recovery, and then reversed. As depicted, the dilated VLDs could be either single or multilobed invaginations. Swelling neurons generated neither membranous blebs nor dye-accessible aqueous compartments. Shrinking neurons sequestered large expanses of surface area by drawing plasma membrane inward at the substratum. In most instances, this drawing-in did not simply elevate areas off the substratum. Rather, each time VLD formed (during repeated osmotic perturbation cycles), they began as ''point invaginations'' which, over the course of several minutes, expanded and penetrated the cytoplasm. As the VLD mouths widened, actipodia formed and then began advancing centripetally (i.e., counter to the direction of widening). The fact that some VLD mouths occluded fully (pinched off) would explain the loss of capacitance (Wan et al., 1995; Dai et al., 1998) in shrinking neurons.

During VLD recovery, actipodia were rimmed by Dil-bright regions at and slightly above the substratum (depicted in Fig. 8*b*, horizontal arrows). Since recovery is inhibited by Brefeldin A (Reuzeau et al., 1995) endocytosing membrane may account for this staining pattern, rather like a macropinocytotic vacuole undergoing endocytosis.

During swelling-induced VLD reversal, hydrostatically driven VLD collapse (depicted in Fig. 8*a* and *c*) evidently preceded the subsequent disappearance of VLD membrane (e.g., Figs. 6 and 7). The ''Dil-stained unit,'' the lipid bilayer, is thin compared to a single confocal slice (<10 nm *vs.* 300–500 nm) so Dil signal from collapsed VLDs may have been one (Fig. 8*c*, right) or several layers (Fig. 8*c*, left). When VLD membrane eventually disappeared completely by reversal in swelling neurons, it presumably rejoined the general plasma membrane, by way of the substratum, as suggested in Fig. 8*c*.

Because swelling molluscan neurons accrue surface membrane with no increase in intracellular calcium (Wan et al., 1995; Herring et al., 1998), high membrane tension engendered by swelling may act directly to recruit membrane and prevent rupture. Others have suggested from electron microscopy in molluscan neurons (Fejtl et al., 1995) that flattened membrane cisternae adjacent to the plasma membrane may be ''hot spots'' of

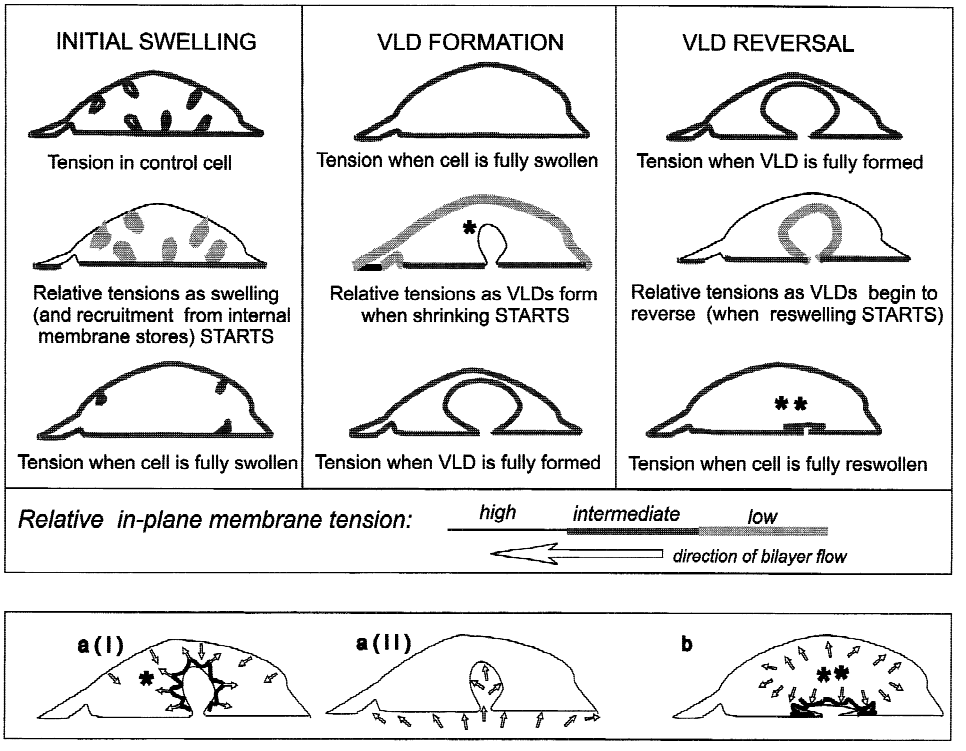

Fig. 9. In-plane tension gradients and VLDs. A swell/shrink/reswell episode is depicted (vertical panels) for a neuron shown in idealized Z-planes. Relative in-plane membrane tension at a given time, in one cell region relative to others, is indicated by line thickness. Tension is equilibrated except after each perturbation (center of each panel). Below, possible impacts of membrane skeleton and hydrostatic pressures (white arrows) on VLD membrane dynamics in shrinking (*a*i, *a*ii) and swelling (*b*) neurons are suggested. The underlying assumption: hydrostatic forces generate nonisotropic membrane tensions so that mechanically contiguous membrane participates in a re-equilibrating bilayer flow. Arbitrarily, a re-equilibrated swollen cell (bottom, left-panel) is depicted with about half its putative tension-accessible internal stores (Fejtl et al., 1995) recruited; subsequently stores are not relevant and so are not depicted. Upon shrinking (center panel), bilayer flow is from dorsum to substratum. Additionally, at discrete sites along the substratum, membrane invaginates (asterisk). VLD initiating sites behave as high tension bilayer sinks. Once formed, VLDs are equilibrium structures (they persist in poisoned cells, Reuzeau et al. (1995)) but osmomechanical work (to re-inflate the cell, right panel) can reverse them; presumably, high tension dorsal membrane becomes a sink for VLD bilayer. A partially reversed VLD is depicted (double asterisks (here and in *b*)), coinciding with observations (Figs. 6 and 7) of compacted VLD membrane. Why do enlarging VLDs act like a high tension sink? Two possibilities are shown in *a*i and *a*ii. In *a*i, membrane skeleton drawn inward with contracting cytoplasm draws bilayer with it. In *a*ii, water exiting at the substratum builds hydrostatic pressure. Though the inflated appearance of VLDs suggests *a*ii, *a*ii wrongly predicts that invaginating VLDs would lack bath dye. (If differences in VLD and bath RD3000 intensities existed in forming VLDs, they were not detectable (*data not shown*)). Moreover, *a*ii (but not *a*i) is incompatible with the findings (Reuzeau et al., 1995) that VLDs formed with actin-based recovery blocked persist indefinitely rather than collapsing, and that VLDs form during prolonged hyposmia. If shrinking cytoplasm draws VLD membrane inwards via a ''plastic'' scaffold (membrane skeleton, as in *a*i), both persistence and the repeatable discrete sites (Figs. 6 and 7) seem explicable. Indeed, VLDs in rat myotubes have a spectrin skeleton (Herring, 1998).

mechanically recruitable membrane. In control neurons, we noted no deeply penetrating membrane invaginations, either with Dil or aqueous phase markers but in confocal microscopy (*see also* Fejtl et al., 1995), subsurface membrane stores may be unresolvable as distinct structures.

Hydrostatic Pressure, In-Plane Membrane Tension and VLDs

For an ideal solid, surface behavior is fully explained by reference to volume behavior. A cell's surface, however, is a discrete entity with mechanics distinct from those of its volume. Thus, osmotic/hydrostatic pressures generate tensions at surface membranes. Neuronal responses to osmotic perturbations such as altered outgrowth patterns (Bray et al., 1991; Wan et al., 1995; Lin et al., 1995) may depend in part on hydrostatically driven membrane tensions. Van Essen (1997) postulates that sustained hydrostatic pressure is a critical tensegrity element for a tension system that optimizes brain wiring. Neurites maintain non-zero tensions critical to outgrowth (Heidemann & Buxbaum, 1994) and regional variations in membrane in-plane tension of neurons affect membrane disposition (Dai & Sheetz, 1995).

Could hydrostatically driven membrane tensions

yield VLD formation and reversal as seen by confocal microscopy? Figure 9 is our working model depicting a relationship between in-plane tension gradients and VLDs. This model is consistent with our confocal microscopy data and with our recent findings (Dai et al., 1998) that membrane tension at the accessible (upper) surface of *Lymnaea* neurons increases with swelling and returns to below control levels upon reshrinking.

VLD Recovery

The cell-mediated process of recovery does not occur in the presence of cytochalasin (Reuzeau et al., 1995), strongly implicating F-actin. Cohan et al. (1997) showed that in cytochalsin-treated neurons, F-actin is absent from VLDs. Here, RD3000 showed that retention of dye in immediately adjacent VLDs differed and Dil experiments showed that some actipodia constricted fully, yielding vacuoles while others remained patent. These findings correlate precisely with ongoing work (Cohan et al., 1997; Herring, 1998) showing that, early during recovery (<5 min), VLD mouths have F-actin rich actipodia whose form coincides with actipodia as revealed by Dil, and that at immediately adjacent actipodia, both the amount of F-actin and the extent of constriction is extremely variable.

Membrane-actin interactions at adhesion sites have been shown in molluscan neurons (Forscher, Lin & Thompson, 1992); polycationic beads bound to the membrane induce rapid assembly of filamentous actin and the production of force. Site-directed actin filament assembly is a widespread cellular mechanism for generating force at membrane-cytoskeletal interfaces (Welch, Iwamatsu & Mitchison, 1997). Actipodia, as revealed by Dil, move centripetally and can pinch off the VLD mouth. The retention of molecules under 0.5 kDa (e.g., LY, MW = 457) in vacuoles confirms that mouths become completely shut off from the bath medium as if by macropinocytosis. In our Dil images, actipodial membrane creeps centripetally under the influence of actin-dependent forces working against the membrane-substratum; appropriately orchestrated, these forces presumably fuse the VLD mouth to create a vacuole.

Regulation of Neuronal Plasma Membrane Surface Area and Membrane Tension

Bilayer rupture is intolerable so cells presumably monitor and counteract elevated membrane tension (Morris et al., 1997). VLDs become evident, we suggest, when a primitive tension-sensitive cell surface area regulation system fails to meet the immediate demands placed on it. VLDs in various guises occur in both plant and animal cells (e.g., Wartenberg et al., 1992; Czekay, Kinne-Saffran & Kinne, 1994). Shrinking frog muscle fibers make VLDs (reversible vacuoles) along their T-tubules (Krolenko, Amos & Lucy, 1995). Rat hippocampal neurons make VLDs that recover within minutes (Dai et al., 1998). Like any cells, neurons, must osmoregulate, but would seldom experience substantial osmotic stimuli. Surface area adjustments would more characteristically be needed in neurons, we suggest, during the remodelling of neuritic processes.

A tension feedback system would be in particularly high demand during neurite outgrowth and during embryogenesis when surrounding tissues impose forces on thin neuronal processes. Later, it could help fine-tune cell shape and provide emergency relief during large tension excursions. Tension-dependent membrane disposition, adjusting membrane area to counter too-high or too-low tension, could be the cell surface counterpart of cytoplasmic tensegrity (Chen et al., 1997). While tension-sensitive exocytosis and endocytosis could deal with small fast adjustments or large slow ones (and indeed, tension modulation of membrane turnover has been noted (Fink & Cooper, 1996; Zorec & Tester 1993)), for emergency responses, rebalancing exocytosis and endocytosis would be too elaborate. A mechanism requiring no intermediary chemical or voltage signals would be more robust and fail-safe.

In neurons, tension-sensitive surface area regulation may go on continually. Multiple VLD-like structures occur in actively reshaping cells (e.g., Fig. 7 of Lin et al., 1996; Cheng & Reese, 1987) and retrieval of growth cone membrane can occur by invagination and pinching off of small vacuoles (Dailey & Bridgman, 1993). Overtax the immediate handling capacity for reprocessing invaginated membrane and the result would likely be a VLD rather than an inconspicuous vesicle.

This work was supported by a grant to CEM and LRM from the Heart and Stroke Foundation of Ontario (ST2716) and by research and equipment grants to CEM and to LRM from NSERC, Canada.

References

Bray, D., Money, N.P., Harold, F.M., Bamburg, J.R. 1991. Responses of growth cones to changes in osmolality of the surrounding medium. *J. Cell Sci.* **98:**507–515

Bray, D. 1996. Membrane biophysics: The dynamics of growing axons. *Current Biology* **6:**241–243

Cohan, C.S., Welnhofer, E.A., Herring, T.L., Morris, C.E. 1997. Actin and filopodial dynamics in osmotically perturbed molluscan neurons. *Mol. Biol. Cell.* **8:**256*a.* (*Abstr.*)

Chen, C.S., Mrksich, M., Huang, S., Whitesides, G.M., Ingber, D.E. 1997. Geometric control of cell life and death. *Science* **276:**1425–1428

Cheng, T.P.O., Reese, T.S. 1987. Recycling of plasmalemma in chick tectal growth cones. *J. Neurosci.* **7:**1752–1759

Czekay, R.P., Kinne-Saffran, E., Kinne, R.K. 1994. Membrane traffic and sorbitol release during osmo- and volume regulation in isolated rat renal inner medullary collecting duct cells. *Eur. J. Cell Biol.* **63:**20–31

Dai, J., Sheetz, M.P. 1995. Axon membrane flows from the growth cone to the cell body. *Cell* **83:**693–701

Dai, J., Sheetz, M.P., Wan, X., Morris, C.E. 1998. Membrane tension in swelling and shrinking molluscan neurons. *J. Neurosci.* **18:**6681–6692

Dailey, M.E., Bridgman, P.C. 1993. Vacuole dynamics in growth cones: correlated EM and video observations. *J. Neurosci.* **13:**3375–3393

Fejtl, M., Szarowski, D.H., Decker, D., Buttle, K., Carpenter, D.O., Turner, J.N. 1995. Three-dimensional imaging and electrophysiology of live *Aplysia* neurons during volume perturbation: confocal light and high-voltage electron microscopy. *J.M.S.A.* **1:**75–85

Fink, R.D., Cooper, M.S. 1994. Apical membrane turnover is accelerated near cell-cell contacts in an embryonic epithelium. *Dev. Biol.* **174:**180–189

Forscher, P., Lin, C.H., Thompson, C. 1992. Novel form of growth cone motility involving site-directed actin filament assembly. *Nature* **357:**515–518

Heidemann, S.R., Buxbaum, R.E. 1994. Mechanical tension as a regulator of axonal development. *Neurotoxicology* **15:**95–108

Herring, T. 1998. Calcium, actin and the spectrin skeleton: responses to swelling and shrinking perturbations. MSc thesis, University of Ottawa

Herring, T.L., Slotin, I.M., Baltz, J.M., Moris, C.E. 1998. Neuronal swelling and surface area regulation: elevated intracellular calcium is not a requirement. *Am. J. Physiol.* **274:**C272–C281

Krolenko, S.A., Amos, W.B., Lucy, J.A. 1995. Reversible vacuolation of the transverse tubules of frog skeletal muscle: a confocal fluorescence microscope study. *J. Muscle Res. Cell Motil.* **16:**401–411

Lin, C., Lamoureux, P., Buxbaum, R.E., Heidemann, S.R. 1995. Osmotic dilution stimulates axonal outgrowth by making axons more sensitive to tension. *J. Biomechanics* **28:**1429–1438

Lin, X-H., Grako, K.A., Burg, M.A., Stallcup, W.B. 1996. NG2 proteoglycan and the actin-binding protein fascin define separate populations of actin-containing filopodia and lamellipodia during cell spreading and migration. *Mol. Biol. Cell* **7:**1977–1993

Mills, L.R., Niesen, C.E., Austin, P.S., Carlen, P., Spigelman, I., Jones, O.T. 1994. N-type Ca^{2+} channels are located on somata, dendrites and a subpopulation of dendritic spines on live hippocampal pyramidal neurons. *J. Neurosci.* **14:**6815–6824

Morris, C.E., Lesiuk, H., Mills, L.R. 1997. How do neuronal processes monitor their mechanical status? *Biol. Bulletin* **192:**118–120

Nichol, J.A., Hutter, O.F. 1996. Tensile strength and dilatational elasticity of giant sarcolemmal vesicles shed from rabbit muscle. *J. Physiol.* **493:**187–198

Reuzeau, C., Mills, L.R., Harris, J.A., Morris, C.E. 1995. Discrete and reversible vacuole-like dilations induced by osmo-mechanical perturbations of neurons. *J. Membrane Biol.* **145:**33–47

Sigurdson, W.J., Morris, C.E. 1989. Stretch-sensitive ion channels in growth cones of snail neurons. *J. Neurosci.* **9:**2801–2808

Sukhorukov, V.L., Arnold, W.M., Zimmerman, U. 1993. Hypotonically induced changes in the plasma membrane of cultured mammalian cells. *J. Membrane Biol.* **132:**27–40

Van Essen, D.C. 1997. A tension-based theory of morphogenesis and compact wiring in the central nervous system. *Nature* **385:**313–318

Wan, X., Harris, J.A., Morris, C.E. 1995. Responses of neurons to extreme osmomechanical stress. *J. Membrane Biol.* **145:**21–31

Wartenberg, M., Hamann, J., Pratsch, I., Donath, E. 1992. Osmotically induced fluid-phase uptake of fluorescent markers by protoplasts of *Chenopodium-album. Protoplasma* **166:**61–66

Welch, M.D., Iwamatsu, A., Mitchison, T.J. 1997. Actin polymerization is induced by ARP/3 protein complex at the surface of *Listeria monocytogenes. Nature* **385:**265–269

Zorec, R., Tester, M. 1993. Rapid pressure driven exocytosis-endocytosis cycle in a single plant cell: capacitance measurements in aleurone protoplasts. *FEBS Lett.* **333:**283–286